Journal of
Materials Chemistry C

Materials for optical, magnetic and electronic devices

Accepted Manuscript

This article can be cited before page numbers have been issued, to do this please use: L. Malavasi, V. Kumar, A. Speltini, L. Romani, A. Bala, A. Profumo, A. Listorti, A. Milella and F. Fracassi, *J. Mater. Chem. C*, 2020, DOI: 10.1039/D0TC02525A.

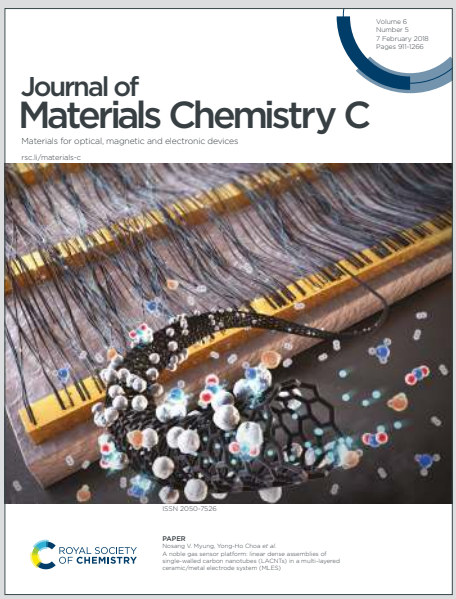

ROYAL SOCIETY OF CHEMISTRY

rsc.li/materials-c

View Article Online
DOI: 10.1039/D0TC02525A

PEA_2SnBr_4: a Water-Stable Lead-Free Two-Dimensional Perovskite and Demonstration of Its Use as Co-Catalyst in Hydrogen Photogeneration and Organic-Dye Degradation

Lidia Romani[a], *Anu Bala,*[b] *Vijay Kumar,*[b,c] *Andrea Speltini,*[d] *Antonella Milella,*[e] *Francesco Fracassi,*[e] *Andrea Listorti,*[e] *Antonella Profumo*[a], *Lorenzo Malavasi*[a,*]

[a]Department of Chemistry and INSTM, University of Pavia, Via Taramelli 12, Pavia 27100, Pavia, Italy

[b]Center for Informatics, School of Natural Sciences, Shiv Nadar University, NH-91, Tehsil Dadri, Gautam Buddha Nagar 201314,Uttar Pradesh, India

[c]Dr. Vijay Kumar Fundation, 1969, Sector 4, Gurgaon 122001, Harayana, India

[d]Department of Drug Sciences, University of Pavia, Via Taramelli 12, Pavia 27100, Pavia, Italy

[e]Department of Chemistry, University of Bari, Via Orabona 4, Bari, 70126, Italy

View Article Online
DOI: 10.1039/D0TC02525A

AUTHOR INFORMATION

Corresponding Author

*Lorenzo Malavasi: lorenzo.malavasi@unipv.it

Keywords: metal organic perovskite, photocatalysis, hydrogen photogeneration, organic dye

ABSTRACT

A novel lead-free 2D perovskite, namely PEA_2SnBr_4, shows an impressive water-resistance by retaining its original crystal structure and optical properties when put in contact with water. Such key properties have been advantageously used in the fabrication of a novel co-catalytic system by coupling PEA_2SnBr_4 with graphitic carbon nitride. PEA_2SnBr_4/g-C_3N_4 composites at different metal halide perovskite loadings (5 and 15 wt%) have been prepared and tested against hydrogen photogeneration in aqueous environment and organic dye degradation (methylene blue). The results shows an impressive enhancement of H_2 production of the composite with respect to the two

View Article Online
DOI: 10.1039/D0TC02525A

separate components with hydrogen evolution rates up to 1600 μmol g^{-1} h^{-1} and analogous improvements in the efficiency of methylene blue degradation. The present results, providing a novel water-resistant perovskite and co-catalytic system, pave the way towards the safe, efficient and real use of metal halide perovskite in catalysis.

Poor water-stability of tridimensional (3D) metal halide perovskites (MHP) is a major concern, and a limit for their application in solar cells technology as well as in

View Article Online
DOI: 10.1039/D0TC02525A

optoelectronic devices.[1-5] Such issue can be overcome by two-dimensional (2D) layered perovskites of general formula $R_2(CH_3NH_3)_{n-1}B_nX_{3n+1}$, where *n* represent the number of inorganic layers, R represents a large organic cation, such as for example $C_6H_5(CH_2)_2NH_3^+$ (phenylethylammonium, PEA), B the metal cation and X the halide. The improved moisture resistance of 2D perovskites comes from the presence of the hydrophobic R groups occupying the surface sites, and protecting the inorganic layers from water.[1] To date, several examples of the use of 2D protecting layers in perovskite solar cells with a 2D/3D architecture have been reported.[2-10] On the other hand, the exceptional optical properties of metal halide perovskites could be used to explore their application in other fields, such as photocatalysis. In this respect, some examples of hydrogen photogeneration by metal halide perovskites is present in the current literature, where the inherent water instability of MHP required the use of concentrated solutions of hydracids (such as HI) to avoid decomposition.[11-15] We have recently shown that it is possible to achieve an improved stability of selected 3D lead-free MHP (namely $DMASnBr_3$, DMA=dimethylammonium) in water where, possibly, the hydrophobic organic group protects the perovskite from both water and tin oxidation, as recently also assessed

View Article Online
DOI: 10.1039/D0TC02525A

from computational modelling.[15,16] Such unexpected water-stability of $DMASnBr_3$ has been also confirmed for the iodide composition.[17] In order to envisage novel applications of MHP, in particular in the photocatalysis field, we have devised a novel 2D lead-free perovskite that could meet the pre-requisite of water stability, suitable optical properties for co-catalysis, and no environmental concerns. As it will be shown below, PEA_2SnBr_4 2D perovskite allowed achieving all these goals, showing an unprecedented water stability that was exploited in the preparation of novel co-catalysts with graphitic carbon nitride (g-C_3N_4), a state-of-the-art material for visible light catalysis.[18-22]

PEA_2SnBr_4 was synthesized by wet-chemistry route in form of bulk material (see details in the Electronic Supplementary Information, ESI) and its x–ray diffraction (XRD) pattern is reported in Figure 1a (bottom part, black curve). The crystal structure agrees with the orthorhombic *Cmca* space group symmetry we defined on the BZA_2SnBr_4 material and the pattern is dominated by (*h*00) reflections, a typical feature of these 2D perovskites[23]. Before preparing the final catalyst, the water stability of the perovskite was tested in two ways: i) by dispersing the powders in distilled water under stirring and

View Article Online
DOI: 10.1039/D0TC02525A

recovering them by filtration; and ii) by measuring the amount of tin into the deionized water (DW) after perovskite removal (leaching test – see ESI for details). Figure 1a (top pattern, blue curve) shows the XRD pattern of PEA_2SnBr_4 after 4 hours in DW under stirring which is superimposable to the starting material, thus confirming that this perovskite does not dissolve in water (also by visual inspection it is possible to note the presence of particles in water). A further comparison of the two patterns is reported in ESI as square root of the intensity, in order to possibly put in prominence very low-amount impurities (Figure S1). Moreover, the leaching test showed that just 0.14 wt% of the starting amount of tin in the perovskite is released in water after 4 h-stirring (see ESI), confirming the exceptional water-stability of this material. The UV-VIS absorbance spectra of the perovskite before (as-prepared) and after water dispersion are reported in Figure 1b and again the absorption-edge remains fixed at 2.67 eV without the appearance of any absorption tail. Defect state associated to Sn^{2+} to Sn^{4+} oxidation is well known to cause a significant change in the optical properties of the MHP.[24] Finally, the strongest proof of water stability comes from the results of X-ray Photoelectron Spectroscopy (XPS) analysis. Figure 1c shows the Sn 3d XPS spectra of as-prepared PEA_2SnBr_4 and after 4

View Article Online
DOI: 10.1039/D0TC02525A

hours in DW under stirring. Binding energies correspond to those of Sn^{2+} (487.6 eV) and as can be seen, the two spectra are superimposable both in terms of position and shape, confirming the extraordinary water-stability of PEA_2SnBr_4 in water and the absence of any oxidation.[25] We remark that a very recent computational modeling work indicates that the presence of PEA hydrophobic groups not only preserve the inorganic layer from water but also protects tin from oxidation.[16] It may be possible that the presence of long and hydrophobic organic groups directly linked to the single inorganic slab create a close and water-repellant environment which protects it both from moisture and in turn to oxidation.

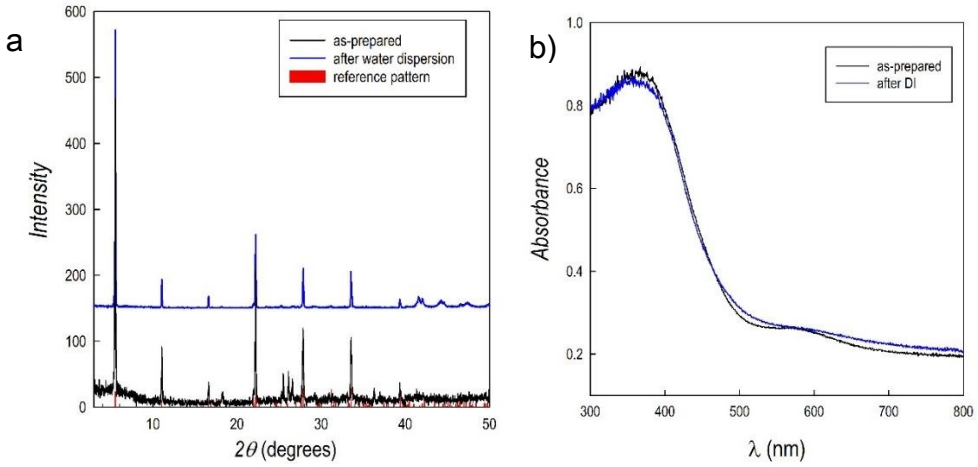

c)

View Article Online
DOI: 10.1039/D0TC02525A

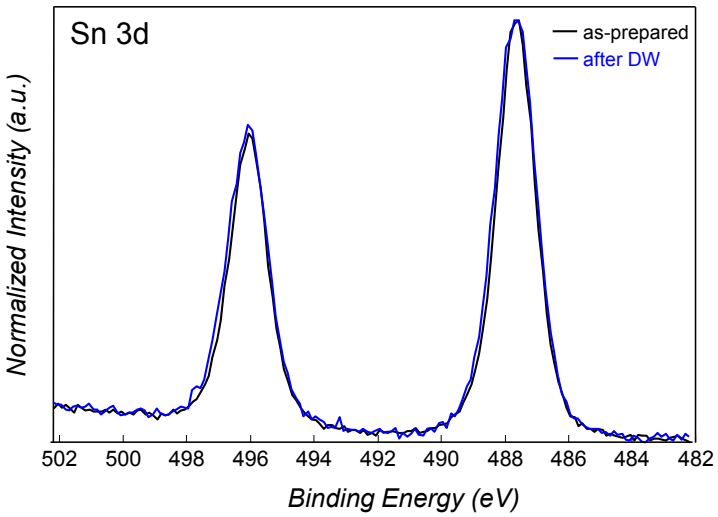

Figure 1. (a) XRD pattern of PEA_2SnBr_4 synthesized by wet-chemistry where red vertical bars refer to the reflection positions for orthorhombic structure of the perovskite: bottom pattern: as-prepared material; top pattern: after recovery from DW; (b) UV-VIS spectra of as-prepared PEA_2SnBr_4 and after recovery from DW; (c) Sn 3d XPS spectra of as-synthesized PEA_2SnBr_4 (black) and after recovery from aqueous solution (blue).

After having assessed the optimal and unprecedented water-stability of PEA_2SnBr_4, we prepared composite catalytic systems by coupling this 2D lead-free perovskite, as a co-catalyst, to g-C_3N_4. This strategy is commonly used for carbon nitride to improve its properties, in particular to increase charge migration and recombination time and to extend the absorption range.[20,21] Common composites are based on the coupling of g-C_3N_4 with metals, bimetals, semiconductors (oxides, sulfides, and the like), graphene, carbon dots, conductive polymers, sensitizers, among others. In this respect,

View Article Online
DOI: 10.1039/D0TC02525A

the unique optical properties of MHPs suggest they can be very good candidates as co-catalysts. In addition, the band-gap of PEA_2SnBr_4 (around 2.67 eV) well matches to that of g-C_3N_4 (2.76 eV) thus suggesting a possible synergic role between the two materials.

PEA_2SnBr_4/g-C_3N_4 composites at different MHP loadings (5 and 15 wt%) were synthesized by wet-chemistry route (see ESI) and their crystal structure characterized by X-ray diffraction (Figure S2, ESI). The composites reveal an overall amorphous-like structure, with the main peak of g-C_3N_4 (around 28°) and the general sample scattering becoming progressively less intense increasing of the amount of metal halide perovskite. No clear diffraction peaks of crystalline perovskites are found in the patterns, suggesting that the presence of g-C_3N_4 during perovskite synthesis tends to reduce the structural order of the PEA_2SnBr_4, also possibly related to the formation of small perovskite particles on the carbon nitride, as revealed by the significant change of morphology passing from pristine g-C_3N_4 to the composite (Figure S3). Energy Dispersive X-ray (EDX) analysis on the composites confirms the homogenous distribution of metal and halide and the expected Sn/Br ratio, ruling out the formation of different phases and/or clustering (Table

View Article Online
DOI: 10.1039/D0TC02525A

S1). XPS spectra of N 1s confirms the presence of quaternary ammonium around 401.4 eV in both composites which is absent in pristine carbon nitride (Figure S4).[26,27] Also the Sn 3d XPS spectra of both composites (Figure S5) shows analogous signals to the starting PEA_2SnBr_4 with a slight shift to lower binding-energies (less than 1 eV) which rules out any oxidation during composite preparation (Sn^{4+} would appear at higher binding energies than Sn^{2+}). The origin of this shift goes beyond the scope of the present paper, and may be related to the interaction between the perovskite and g-C_3N_4 as well as to the peculiar morphology of the composites and will be object of future work.

Optical absorbance spectra of PEA_2SnBr_4/g-C_3N_4 composites (Figure 2a) show the expected predominance of g-C_3N_4 feature for both 5 and 15% perovskite loadings, by keeping the absorbance threshold around 2.76 eV (see Tauc plots in ESI, Figure S6). This result could also be anticipated considering the relatively small difference in the band-gap between carbon nitride and PEA_2SnBr_4.

View Article Online
DOI: 10.1039/D0TC02525A

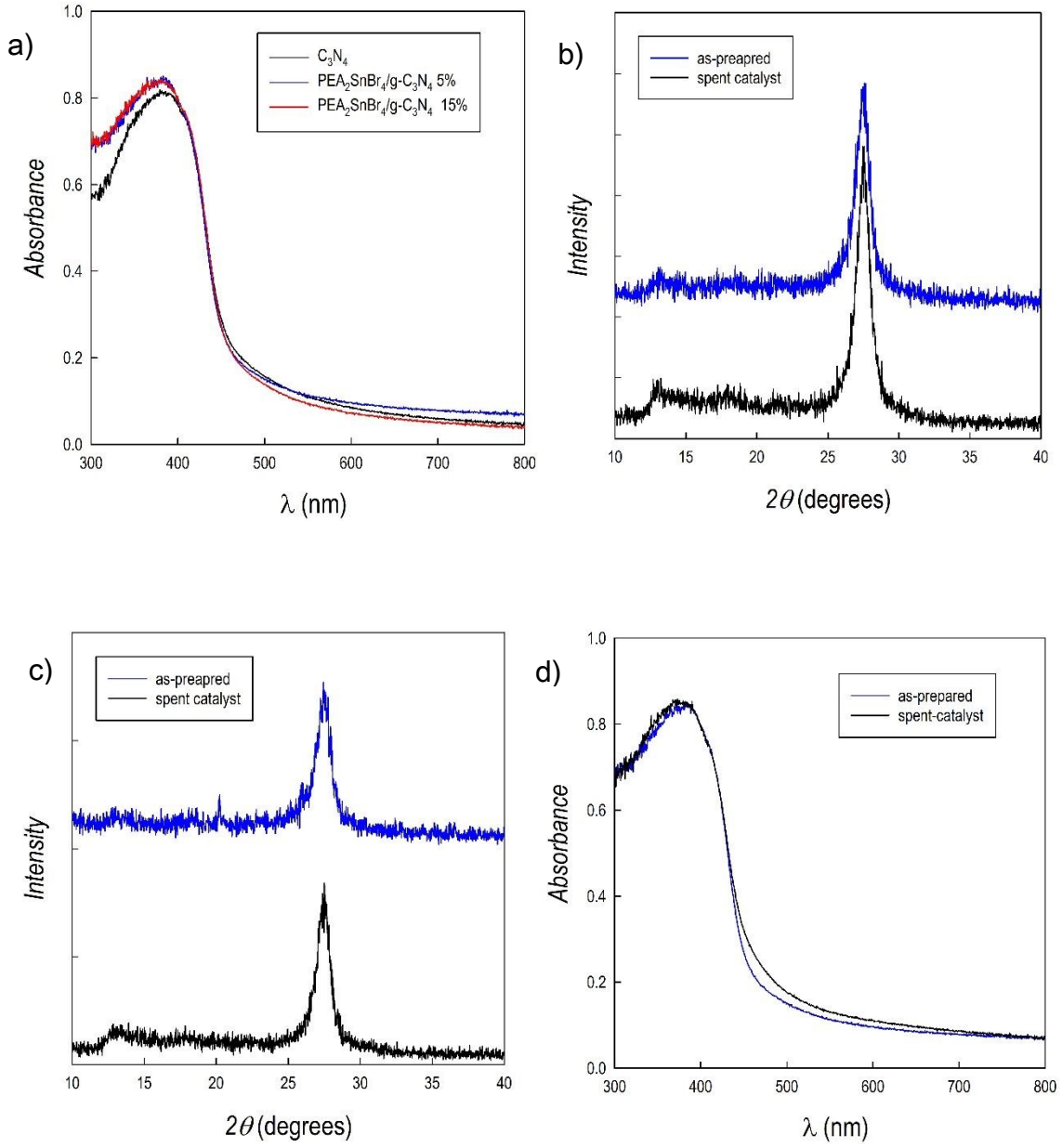

Figure 2. (a) UV-Vis spectra of pristine g-C_3N_4 and $PEA_2SnBr_4/g\text{-}C_3N_4$ composites; (b) XRD pattern of $PEA_2SnBr_4/g\text{-}C_3N_4$ 5% composite as-prepared and after H_2 photogeneration experiment (spent catalyst); (c) XRD pattern of $PEA_2SnBr_4/g\text{-}C_3N_4$ 15% composite as-prepared and after H_2 photogeneration experiment (spent catalyst); d) UV-Vis spectra of $PEA_2SnBr_4/g\text{-}C_3N_4$ 5% composite as-prepared and after H_2 photogeneration experiment (spent catalyst).

View Article Online
DOI: 10.1039/D0TC02525A

Once the pure perovskite and the composites have been characterized, we focused on the evaluation of their photocatalytic properties, by looking at hydrogen photogeneration from water and degradation of model organic water pollutants, by employing common protocols used for similar g-C_3N_4-based composites.[22] The results reported in the following have been performed on several replicas of the composites and the experimental details of the hydrogen evolution tests are reported in the Experimental Section (ESI).

Firstly, hydrogen photogeneration efficiency of the PEA_2SnBr_4/g-C_3N_4 composites (5 and 15 wt% of perovskites with respect to g-C_3N_4) has been determined in water containing10% triethanolamine (TEOA), as a typical sacrificial agent, and with a 3 wt% Pt loading. We stress that these are the conditions used to test all the carbon nitride-based materials as it can be inferred from refs. 14-18. The H_2 evolution rates (HERs) as a function of perovskite loading of the composites are reported in Table 1.

Table 1. HERs from aqueous solutions for g-C_3N_4 and PEA_2SnBr_4/g-C_3N_4 composites at different percentages of metal halide perovskite loading as well as for PEA_2SnBr_4 (1 g L^{-1} catalyst, 3 wt% Pt, 6 h irradiation under simulated solar light, 500 W m^{-2}).). In parentheses the standard deviation is reported (RSD $\leq$ 10%, n=3).

View Article Online
DOI: 10.1039/D0TC02525A

	HER (μmoles g^{-1} h^{-1})	
	10% TEOA	0.1 M Glucose
PEA_2SnBr_4	4(0.4)	< 0.1
$PEA_2SnBr_4/g\text{-}C_3N_4$ 5%	1613(98)	107(8)
$PEA_2SnBr_4/g\text{-}C_3N_4$ 15%	963(59)	n.d.
$g\text{-}C_3N_4$	81(6)	3(0.3)

n.d., not determined

From the data reported in Table 1, it is possible to make several considerations: i) a hydrogen production (4 μmol g^{-1} h^{-1}) is observed for the perovskite alone; ii) $g\text{-}C_3N_4$ shows a significant HER of 81 μmoles g^{-1} h^{-1}; iii) an impressive synergic effect is observed

View Article Online
DOI: 10.1039/D0TC02525A

for both composites, providing HERs which are more than 20 and 10 times that of pure carbon nitride for a perovskite loading of 5 and 15%, respectively; iv) comparing the data of pure g-C_3N_4 and that of the two composites, it is possible to suggest a optimal loading of the PEA_2SnBr_4 around 5 wt%. Finally, a HER of about 1600 μmol g^{-1} h^{-1} for the PEA_2SnBr_4/g-C_3N_4 composite with 5% of perovskite places it close to the materials with ultra-high HER.[22] Table 1 reports also the effectiveness of PEA_2SnBr_4/g-C_3N_4 (5 wt% perovskite – best performing composite) for the photogeneration activity in 0.1 M aqueous glucose, representative of a biomass-derived sacrificial agent. The HER for the composite was 107 μmol g^{-1} h^{-1} and that of pure g-C_3N_4 was 3 μmol g^{-1} h^{-1}, i.e. a 30-fold improvement. To check the stability of the PEA_2SnBr_4/g-C_3N_4 composites after photogeneration reaction, the reaction solution was filtered and the powder recovered and subjected to XRD and UV-Vis spectroscopy. The patterns of the composites before and after the photocatalytic tests are reported in Figures 2b and 2c, showing unaltered patterns of the spent catalysts compared to the starting material. No evidence of reduction products (e.g. elemental tin) were found in the patterns, confirming the stability of the composites. Moreover, compared to the as-prepared powder also the UV-Vis spectra remain unchanged for the

View Article Online
DOI: 10.1039/D0TC02525A

spent catalyst (Figure 2d for 5 wt%, as selected example). Finally, EDX analysis performed on it confirmed the preservation of the Sn/Br ratio of the 2D perovskite in the composite.

The composite with higher HER was also tested to check its activity towards the decomposition of organic dyes, by selecting methylene blue (MB) as a representative model compound of this class. Figure 3 shows the trend of MB concentration (plotted as C/C_0, where C_0 is the initial concentration) as a function of irradiation time, compared to pure g-C_3N_4 and direct photolysis (see details in the ESI).

View Article Online
DOI: 10.1039/D0TC02525A

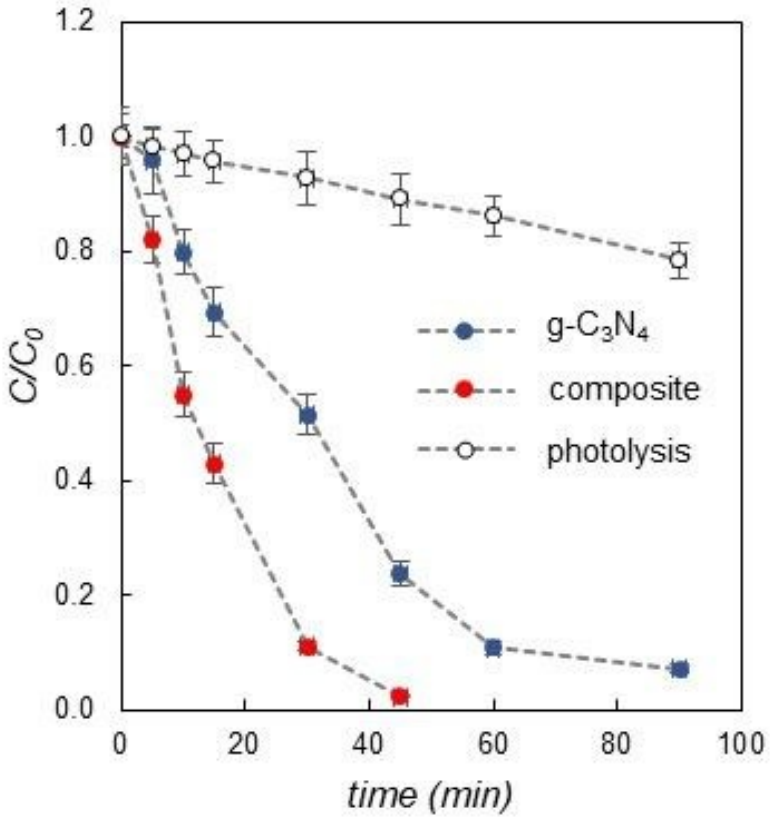

Figure 3 Variation of MB concentration as a function of irradiation time for g-C_3N_4 (blue dots) and PEA_2SnBr_4/g-C_3N_4 5% composite (red tots), compared to photolysis effect (empty dots); conditions: 1 g L^{-1} catalyst, 250 W m^{-2} simulated solar light. RSD < 10% (n=3).

It is clear from the Figure above, as it occurs for the hydrogen photogeneration, that the reported novel composite performs better than pure carbon nitride also with respect to organic dye degradation. In particular, pristine g-C_3N_4 cannot completely

View Article Online
DOI: 10.1039/D0TC02525A

degrade MB even after 90 minutes of irradiation, while the PEA_2SnBr_4/g-C_3N_4 composite completely decomposes the dye in about 40 minutes.

The particularly efficient performance of the PEA_2SnBr_4/g-C_3N_4 composite can be understood on the basis of the relative band-alignment of the two semiconductors when present in the composite.

The valence band maximum (VBM) and conduction band minimum (CBM) edge positions of g-C_3N_4 and PEA_2SnBr_4 relative to the NHE potential were calculated using the work function method:

$$E_{VBM} = -\Phi - 0.5\,E_g$$

$$E_{CBM} = -\Phi + 0.5\,E_g$$

$$E'_{CBM(VBM)} = -E_{CBM(VBM)} - 4.5$$

where Φ is the work functions defined as the minimum energy required to extract an electron from a material, and is equal to the energy difference between the Fermi level and the electrostatic potential energy in vacuum. Further E_g is the band gap and $E'_{CBM(VBM)}$ is the potential vs. NHE, and are reported in Figure 4.[28,29] The calculated Φ's of g-C_3N_4 (optimized structure Figure S7) and PEA_2SnBr_4 (optimized structure Figure S8) using HSE06 functional are 4.61 eV (Figure S9) and 4.14 eV (Figure S10), respectively. Notably, the calculated E_g values with HSE06 for g-C_3N_4 (2.8 eV) and PEA_2SnBr_4 (2.74 eV) monolayers are in good agreement with experimental values of 2.76 eV and 2.67 eV, respectively. As depicted in Figure 4, the CBM of g-C_3N_4 and PEA_2SnBr_4 are at

View Article Online
DOI: 10.1039/D0TC02525A

-1.29 V and −1.74 V vs. NHE which are above the H^+/H_2 potential whereas the VBM of g-C_3N_4 are at 1.51 V vs. NHE below the O_2 potential. Since the band gap values of both the semiconductors are comparable, the electron-hole pairs are generated in both the semiconductors under visible-light irradiation. As a consequence of the band alignment shown in Figure 4, the photo induced electrons from PEA_2SnBr_4 can easily move towards g-C_3N_4 due to CBM lying at less negative potential. Finally, the accumulated electrons take part in the photochemical reduction of water to generate hydrogen. In such a way, the hetero-junction formed could limit the recombination rate of photo generated electron-hole pairs thus remarkably increasing the photocatalytic activity for hydrogen evolution than that of pure g-C_3N_4.

View Article Online
DOI: 10.1039/D0TC02525A

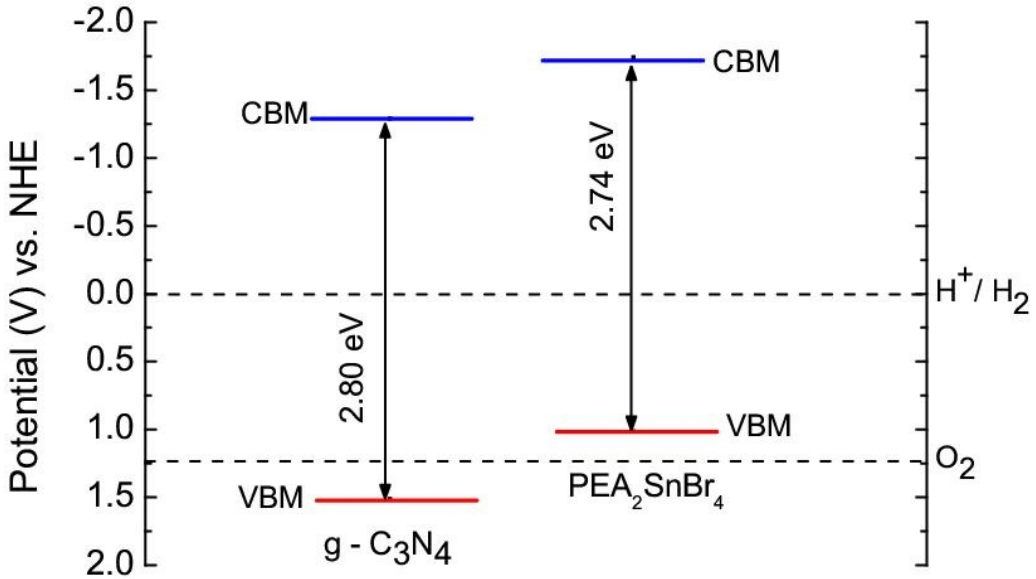

Figure 4: Calculated band edge positions (solid lines) for two semiconductors relative to NHE potential. The two dashed lines indicate the water redox reaction potentials

View Article Online
DOI: 10.1039/D0TC02525A

Conclusion

A novel 2D lead-free metal halide perovskite, PEA_2SnBr_4, has been synthesized and characterized, showing an impressive and unprecedented water-resistance in both structural and optical properties. Such features have been exploited in the preparation of novel co-catalytic systems by coupling PEA_2SnBr_4 with g-C_3N_4 due to the close band-gap of the two semiconductors. The composites synthesized showed an impressive synergic effect in the enhancement of photocatalytic hydrogen production in aqueous environment as well as in the degradation of organic dyes, without any degradation observed in the spent catalyst. Computational modelling provides a description of the favorable band-alignment between PEA_2SnBr_4 and g-C_3N_4, thus confirming the synergic role from a microscopic point of view. The discovery of water-stable metal halide perovskite allows exploring new applications of these materials, taking advantage of their superior optical properties, in catalysis under experimental conditions which have not been possible up to now.

View Article Online
DOI: 10.1039/D0TC02525A

ASSOCIATED CONTENT

Electronic Supplementary Information. Further experimental data, SEM and X-ray diffraction. Experimental and Computational details

AUTHOR INFORMATION

View Article Online
DOI: 10.1039/D0TC02525A

Lorenzo.malavasi@unipv.it

ACKNOWLEDGMENT

A.B. acknowledges financial support from the Department of Science and Technology (DST), Government of India, through the Project Grant No. SR/WOS-A/PM-1042/2015. The calculations have been performed using the High-Performance Computing facility MAGUS of Shiv Nadar University. L.M. acknowledge the financial support of R.S.E.

REFERENCES

View Article Online
DOI: 10.1039/D0TC02525A

(1) P. Gao, A. R. B. M., Yusoff, M.K. Nazeeruddin, Nature Comm., 2018, **9**, 5028.

(2) H. Xu, Y. Sun, H. Zheng, G. Liu, X. Xu, S. Xu, L. Zhang, X. Chen, X. Pan, J. Mater. Chem. C 2019, **7**, 15276-15284.

(3) J. Schlipf, Y. Hu, S. Pratap, L. Biessmann, N. Hohn, L. Porcar, T. Bein, P. Docampo, P. Muller-Buschbaum, ACS Appl. Energy Mater. 2019, **2**, 1011-1018.

(4) I. C. Smith, E.T. Hoke, D. Solis-Ibarra, M.D. McGehee, H. I. A. Karunadasa, Angew. Chem. 2014, **126**, 11414–11417.

(5) Y. Hu, T. Qiu, F. Bai, W. Ruan, S. Zhang, Adv. Energy Mater. 2018, **8**, 1703620.

(6) A. Z. Chen, M. Shiu, J. H. Ma, M. R. Alpert, D. Zhang, B. J. Foley, D.-M. Smilgies, S.-H. Lee, J. J. Choi, Nat. Commun. 2018, **9**, 1336.

(7) D. H. Cao, C.C. Stoumpos, O.K. Farha, J.T. Hupp, M. G. Kanatzidis, J. Am. Chem. Soc. 2015, **137**, 24.

(8) H. Tsai, W. Nie, J.-C. Blancon, C.C. Stoumpos, R. Asadpour, B. Harutyunyan, A.J. Neukirch, R. Verduzco, J.J. Crochet, S. Tretiak, L. Pedesseau, J. Even, M.A. Alam, G. Gupta, J. Lou, P.M. Ajayan, M.J. Bedzyk, M.G. Kanatzidis, A.D. Mohite, Nature 2016, 536, 312-316.

View Article Online
DOI: 10.1039/D0TC02525A

(9) L.N. Quan, M. Yuan, R. Comin, O. Voznyy, E.M. Beauregard, S. Hoogland, A. Bunin, A. R. Kirmani, K. Zhao, A. Amassian, D.H. Kim, E.H. Sargent, J. Am. Chem. Soc. 2016, 138, 2649-2655.

(10) T. Ming Koh, V. Shanmugam, X. Guo, S. S. Lim, O. Filonik, E. M. Herzig, P. Mueller-Buschbaum, V. Swamy, S. T. Chien, S. G. Mhaisalkar, N. Mathews, J. Mater. Chem. A 2018, 6, 2122-2128.

(11) Z. Zhao, J. Wu, Y.-Z. Zheng, N. Li, X. Li, X. Tao, ACS Catal. 2019, **9**, 8144-8152.

(12) S. Park, W. J. Chang, C. W. Lee, S. Park, H.-Y. Ahn, K. T. Nam, Nature Energy 2016, **2**, 16185.

(13) M. Wang, Y. Zuo, J. Wang, Y. Wang, X. Shen, B. Qiu, L. Cai, F. Zhou, S. P. Lau, Y. Chai, Adv. Energy Mater 2019, **9**, 1901801.

(14) Z. Zhao, J. Wu, Y.-Z. Zheng, N. Li, X. Li, Z. Ye, S. Lu, X. Tao, C. Chen, Appl. Catal. B 2019, **253**, 41-48.

View Article Online
DOI: 10.1039/D0TC02525A

(15) A. Pisanu, A. Speltini, P. Quadrelli, G. Drera, L. Sangaletti, L. Malavasi, J. Mater. Chem. C 2019, **7**, 7020.

(16) A. Bala, V. Kumar, J. Phys. Chem. C 2019, **123**, 25176-25184.

(17) D. Ju, X. Zheng, J. Liu, Y. Chen, J. Zhang, B. Cao, H. Xiao, F. O. Mohammed, O. M. Bakr, X. Tao, Angew. Chem. Int. Ed. 2018, **57**, 14868-14872.

(18) S. Cao, J. Low, J. Yu, M. Jaroniec, Adv. Mater. 2015, **27**, 2150-2176.

(19) S. Ye, R. Wang, M.-Z. Wu, Y.-P. Yuan, Appl. Surf. Sci. 2015, **358**, 15-27.

(20) Z. Zhao, Y. Sun, F. Dong, Nanoscale 2015, **7**, 15.

(21) N. Fajrina, M. A. Tahir, Int. J. Hydr. Energy 2019, **44**, 540-577.

(22) G. Liao, Y. Gong, L. Zhang, H. Gao, G.-J. Yang, B. Fang, Energy Environ. Science 2015, **7**, 15.

(23) A. Pisanu, M. Coduri, M. Morana, Y. O. Ciftci, A. Rizzo, A. Listorti, M. Gaboardi, L. Bindi, V. I. E. Queloz, C. Milanese, G. Grancini, L. Malavasi, J. Mater. Chem. A 2020, **8**, 1875-1886.

View Article Online
DOI: 10.1039/D0TC02525A

(24) T. B. Song, T. Yokoyama, C. C. Stoumpos, J. Logsdon, D. H. Cao, M. R. Wasielewski, S. Aramaki, M. G. Kanatzidis, J. Am. Chem. Soc. 2017, **139**, 836-842.

(25) Hou L., Zhu Y., Zhu J., Li C. Tuning Optical Properties of Lead-Free 2D Tin-Based Perovskites with Carbon Chain Spacers. *J. Phys. Chem. C* **2019**, 123, 31279.

(26) Lan Z.-A., Zhang G., Wang X. A facile synthesis of Br-modified g-C_3N_4semiconductors forphotoredox water splitting. *Appl. Catal. B* **2016**, 192, 116.

(27) Beamson G., Briggs D. High Resolution XPS of Organic Polymers - The Scienta ESCA300 Database Wiley Interscience **1992**, 278.

(28) O. Francis, K. G. Krishna, G. C. E. Cornelia, P. G.Penny, Appl. Surf. Sci. 2018, **427**, 487−498.

(29) K.K. Dalal, A. C. Emily, J. Phys. Chem. C. 2012, **116**, 9876−9887.

View Article Online
DOI: 10.1039/D0TC02525A

ToC

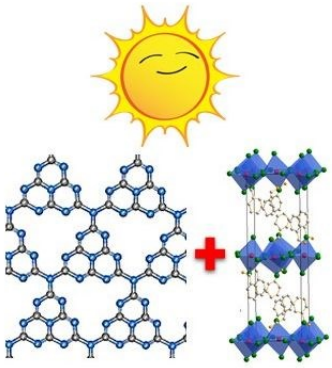

Novel 2D lead-free perovskite showing stability in water and providing efficient hydrogen photogeneration